Supplemental Materials and Methods

$G\alpha_{12}$ ablation exacerbates liver steatosis and obesity by suppressing USP22/SIRT1-regulated mitochondrial respiration

Tae Hyun Kim, Yoon Mee Yang, Chang Yeob Han, Ja Hyun Koo, Hyunhee Oh, Su Sung Kim, Byoung Hoon You, Young Hee Choi, Tae-Sik Park, Chang Ho Lee, Hitoshi Kurose, Mazen Noureddin, Ekihiro Seki, Yu-Jui Yvonne Wan, Cheol Soo Choi, and Sang Geon Kim

Supplementary Materials and Methods

Materials

Antibodies directed against $G\alpha_{12}$ (sc-409, sc-515445), IDE (sc-393887), and PGC1 (sc-13067) were purchased from Santa Cruz Biotechnology (Santa Cruz, CA). Antibody against $G\alpha_{12}$ (orb4561, for immunoblotting of human liver samples) was purchased from Biorbyt (Cambridge, UK). Anti-SIRT1 (8469), anti-SIRT3 (2627), anti-Akt (4685), anti-phospho Akt (Ser473) (9271), and anti-phospho Akt (Thr308) (9275) antibodies were supplied from Cell Signaling Technology (Danvers, MA), whereas anti-SIRT5 (ab78982) and anti-UCP1 (ab10983) antibodies were from Abcam (Cambridge, UK). Anti-HIF-1α antibodies were purchased from either BD Biosciences Pharmingen (San Jose, CA) (610958) or Santa Cruz Biotechnology (sc-13515). Anti-USP22 antibody (NBP1-49644) was provided from Novus Biologicals (Littleton, CO). Anti-β-actin antibody (A5441), anti-ubiquitin antibody (U0508), cycloheximide, erythro-9-(2-hydroxy-3-nonyl)adenine, dipyridamole, C3 toxin (a8724), palmitate and bovine serum albumin were supplied from Sigma-Aldrich (St. Louis, MO). Horseradish peroxidase-conjugated goat anti-rabbit (G21234) and goat anti-mouse IgGs (G21240) were purchased from Invitrogen (Carlsbad, CA). Mouse anti-carnitine palmitoyl transferase-1 (CPT1) antibody (15184-1-AP) was supplied from Proteintech (Chicago, IL). Antibodies obtained from Santa Cruz Biotechnology were used at a ratio of 1:1000 dilution, whereas the others were done in 1:5000-10000 dilution. [^{3}H]-palmitate was obtained from Perkin-Elmer (Waltham, MA). MG132 and SP600125 (JNK inhibitor) were provided from Calbiochem (La Jolla, CA). Y-27632, N6-cyclopentyladenosine, and Cl-IB-MECA were purchased from Tocris Biosciences (Bristol, UK), whereas CGS-21680 and NECA were obtained from Sigma-Aldrich (St. Louis, MO).

Histological Analysis

Paraffin-embedded liver, white adipose tissue, or brown adipose tissue sections were stained with hematoxylin and eosin for tissue morphology. Frozen liver tissues were stained with Oil red O for neutral TG and lipids.

Triglyceride Measurement

Samples of mouse liver (0.3 g) were homogenized in 0.1 M Tris–acetate buffer (pH 7.4) containing 0.1 M potassium chloride and 1 mM EDTA. Six volumes of chloroform/methanol (2:1) were then added. After vigorous stirring, the mixtures were incubated on ice for 1 h and then centrifuged at 800 g for 3 min. The resulting lower phase was aspirated. The TG content was determined using Sigma Diagnostic Triglyceride Reagents (Sigma, St. Louis, MO) (1).

Serum Biochemical Analysis

Serum alanine aminotransferase (ALT), aspartate aminotransferase (AST), lactate dehydrogenase (LDH) activities, TG, free fatty acid (FFA) and total cholesterol levels were analyzed using Spectrum, an automatic blood chemistry analyzer (Abbott Laboratories, Abbott Park, IL). Fasting glucose and insulin contents in serum were measured using Accu-Chek Active (Roche, Germany) and Ultra-Sensitive Mouse Insulin ELISA kits (Crystal Chem, Downers Grove, IL), respectively. C-Peptide, adiponectin, and leptin levels were assessed using Mouse C-Peptide ELISA, Mouse HMW & Total Adiponectin ELISA, and Mouse/Rat Leptin ELISA (Alpco Diagnostics, Salem, NH), respectively. Serum IL-6 and resistin were measured using Mouse IL-6 Quantikine ELISA kit and Mouse Resistin Quantikine ELISA kit (R&D Systems, Minneapolis, MN). Serum TNFα was determined using Mouse TNF alpha ELISA kit (Pierce, Rockford, IL).

Microarray Analysis

Eight-week-old male WT and *Gna12* KO mice were maintained on normal chow diet (ND) and fasted overnight before sacrifice. Total RNA was extracted from three pairs of WT and *Gna12* KO mouse liver using RNeasy Mini kit (Qiagen, Valencia, CA) for hybridization to Agilent Whole Mouse Genome Microarray 8×60k platform (Agilent Technologies, Inc., Santa Clara, CA), as previously reported (2). Microarray data was normalized using GeneSpring GX software (Agilent Technologies). Among the genes differently expressed by *Gna12* KO, the candidate genes were narrowed down by

the criteria of *P* values < 0.05 and a fold-change >2, and genes of interest were categorized into multiple biological pathways using Ingenuity Platform Analysis software. Gene ontology clustering analysis was performed using either PANTHER ver.11 (3) or DAVID 6.7 software (4, 5). Gene interaction analysis between the clustered genes was achieved according to STRING ver.9.1 database (6). Further visualization was done by Cytoscape 3.0.0 software (GEO accession code: GSE51694) (7).

Primary Hepatocyte Isolation and Cell Culture

Mouse primary hepatocytes were isolated under the guidelines of the institutional animal use and care committee, as described previously (8). For cell lines, HepG2 and AML12 cells were purchased from American Type Culture Collection (Rockville, MD). WT or $G\alpha_{12}$-deficient mouse embryonic fibroblast (MEF) cells were kindly provided by Dr. Melvin I. Simon (California Institute of Technology, Pasadena, CA) (9). Min6 cells (a mouse insulinoma-derived cell line) were kindly provided by Dr. Eun Young Park (Mokpo National University, Mokpo, Korea). HepG2 and the MEF cells were maintained in the DMEM containing 10% FBS, 50 units/ml penicillin, and 50 μg/ml streptomycin, whereas AML12 cells were cultured in the DMEM/F-12 containing 10% FBS, insulin-transferrin-selenium X (ITSX), dexamethasone (40 ng/ml; Sigma), and the antibiotics. Min6 cells were grown in DMEM containing 15% FBS, 2.5 mM β-mercaptoethanol, 50 units/ml penicillin, and 50 μg/ml streptomycin. The cells with less than 20 passage numbers were used.

Measurement of Mitochondrial Oxygen Consumption Rate

Oxygen consumption rate (OCR) was assessed using liver mitochondrial fractions prepared from WT or *Gna12* KO mice subjected to fasting overnight (10). After isolation of mitochondrial fractions, protein concentrations in each set of samples were assessed by the Bradford method, as reported previously (1). Mitochondrial OCR was calculated as an amount of oxygen consumed during a certain period of time normalized with protein contents for each sample using Clark-type electrode in a

continuously stirred sealed and thermostatically controlled chamber maintained at 37.8°C (Oxytherm System, Hansatech Instruments Ltd., Norfolk, UK).

For cell-based OCR assays, AML12 cells were infected with Ad-SIRT1 (or Ad-Con) for 16 h and seeded in XF96 microplates at 20,000 cells per well. One hour prior to the assay, cells were washed with XF assay base medium and placed into non-CO_2 incubator maintained at 37°C. OCR was measured using XFe96 Extracellular Flux Analyzer (Seahorse Bioscience) according to the manufacturer's instruction. In addition to the basal respiration, several parameters of mitochondrial respiration were assessed by sequential additions of oligomycin (1 μM, ATP synthase inhibitor), FCCP (1 μM, chemical uncoupler), and rotenone plus antimycin A (0.5 μM each, Complex I and III inhibitors, respectively).

Palmitate β-Oxidation

Primary hepatocytes were isolated and seeded at a density of 5×10^5 per well in 12 well-plates. Palmitate oxidation was measured according to the published methods (11, 12). Briefly, hepatocytes were maintained in a medium supplemented with [9,10-^{3}H]palmitate complexed to BSA by vortexing a mixture of the palmitate and a 10% BSA solution at a 1:2 volume ratio. A total of 3.3 μl [9,10-^{3}H]palmitate and 6.7 μl BSA were used per 1 ml of cell culture medium. After cell culture in a 12-well plate for 24 h, supernatant was applied to ion-exchange column (Dowex 1×8-200, Sigma), and tritiated water was recovered by eluting with 2.5 ml H_2O. A 0.75-ml aliquot was used for scintillation counting.

Hydrodynamic Injection of Plasmid in Mice

For the in vivo experiments, shRNA-expressing plasmid against mouse $G\alpha_{12}$ (sh-$G\alpha_{12}$) and non-targeting control luciferase (sh-Luci) (2, 13) were prepared using Endofree-plasmid mega kit (Qiagen, Hilden, Germany). After 1 week of acclimation, 8-week-old C57BL/6 mice were hydrodynamically injected with sh-$G\alpha_{12}$ or sh-Luci plasmid DNA (50 μg each plasmid) through tail vein. In another

experiment, a plasmid encoding for USP22 (Addgene plasmid #22575, a gift from Dr. Wade Harper) (14) or control plasmid (MSCV-GFP) was prepared in an identical procedure. WT and *Gna12* KO mice at 12 weeks of age were hydrodynamically injected with USP22 or control plasmid DNA (30 μg each) via tail vein. For both experiments, a total volume equivalent to 10% of the mouse body weight in PBS was delivered within 5-7 seconds. Five days after the injection, ad libitum-feeding or fasting for 24 h was conducted as described in the Materials and Methods.

Target Gene Delivery

Adenovirus encoding for mouse $G\alpha_{12}QL$ (Q229L) was kindly provided from Dr. Patrick J. Casey (Duke University Medical Center, Durham, NC). For lentivirus encoding $G\alpha_{12}$, the mouse albumin enhancer/promoter (NB) construct was kindly provided by Dr. Richard D. Palmiter (University of Washington) (15). The original EF1 promoter of pCDH-EF1-MCS-copGFP plasmid (System Biosciences) was replaced with the albumin enhancer/promoter. The coding region of pcDNA3-$G\alpha_{12}$, a gift from Dr. Danny N. Dhanasekaran (The University of Oklahoma Health Sciences Center), was extracted and cloned downstream of the albumin enhancer/promoter. The constructs were sequenced to assess the integrity of insert. HEK293T cells were co-transfected with the plasmids and packaging vectors to generate viral particles. For in vivo experiments, 100 μl of 1.5×10^7 TU was administered to 8-week-old C57BL/6 mice via tail vein. For SIRT1 overexpression in vivo, adenovirus expressing mouse SIRT1 (Ad-SIRT1, 2.8×10^9 PFU/mouse) (Vector Biolabs, Philadelphia, PA) was injected to 15-week-old male WT or *Gna12* KO mice via tail vein. Ad-SIRT1 used for in vitro experiments was generously provided by Dr. Junichi Sadoshima (Rutgers New Jersey Medical School, Newark, NJ). For both in vitro and in vivo assays using adenovirus, Ad-GFP was used as an infection control.

Palmitate Preparation and Treatment

Palmitate solution (final concentration at 1 mM) was prepared as previously described (1). After serum starvation overnight, primary hepatocytes isolated from *Gna12* KO mice were incubated with

500 μM palmitate for 18 h. The cells were then washed with PBS, fixed with 10% formalin for 1 h, and stained with Oil Red O prior to visual inspection (16). For immunoblotting assays, cells were treated with 500 μM palmitate for 24 h (Min6 cells) or 36 h (AML12 cells).

MTT Assays

AML12 cells were used to assess palmitate-induced cytotoxicity using MTT assays, as described previously (17). Briefly, the cells seeded at a density of 1×10^5 cells per well in a 48-well plate were cultured until 70-80% confluency. Cells were treated with 500 μM palmitate for 48 h, and viable cells were stained with MTT reagent (Sigma, 0.25 mg/ml for 1-2 h). After the removal of culture media, the formazan crystals produced in the wells were dissolved in DMSO to measure the absorbance at 590 nm using a microplate reader (SpectraMax I3X, Molecular Devices, Sunnyvale, CA).

Insulin Secretion Assay

Min6 cells infected with either Ad-Gα_{12}QL or Ad-Con were transferred and cultured in 48 well-plate until 80-90% confluency. The cells were treated with 500 μM palmitate for 24 h in the presence or absence of chemical JNK inhibitor (SP600125, 20 μM), followed by incubation for 1 h with Krebs-Ringer bicarbonate HEPES (KRBH) buffer without FBS prior to stimulation with high glucose (25 mM) in the same KRBH buffer. After high glucose stimulation for 1 h, 100 μl of the supernatant was collected and stored in a deep freezer at -70°C until use. The medium was diluted 1:40 with KRBH buffer without BSA and analyzed for insulin content using an Ultrasensitive Mouse Insulin ELISA kit (Crystal Chem, Downers Grove, IL) according to the manufacturer's instruction. The content of insulin secreted into the culture media for each sample was normalized to cellular protein concentration.

Analysis of Energy Balance

Food consumption, energy expenditure, respiratory quotient, oxygen consumption, and locomotor

activity were assessed in a metabolic monitoring system (CLAMS: Columbus Instruments) for 4 days (3 days of acclimation followed by 1 day measurement) prior to (9-week-old) and after 4 weeks (13-week-old) of HFD feeding. Locomotor activity was measured by counting the number of infrared beam breaks on x- and z-axes during the measurement period, as previously described (18). Rectal temperature was measured using a MSR Digital Thermometer (Measure Technology, Taipei Hsien, Taiwan).

Glucose Tolerance and Insulin Tolerance Tests

Mice fed HFD for 13 weeks were fasted overnight and then gavaged with glucose (2 g/kg body weight) for glucose tolerance test. After two weeks of recovery with HFD supplementation, the mice were fasted for 4 h and received an intraperitoneal injection of insulin (Humalog, 0.75 IU/kg body weight) for insulin tolerance test. For each experiment, blood samples were taken from tail vein and blood glucose levels in the samples were measured using an Accu-Check glucometer (Roche) at 0, 30, 60, and 120 min after treatment. Experiments were repeated twice and similar results were obtained.

Hyperinsulinemic-Euglycemic Clamp Study

Seven days prior to the hyperinsulinemic-euglycemic clamp studies, indwelling catheters were placed into the right internal jugular vein extending to the right atrium. After fasting overnight, [3-^{3}H]glucose (HPLC purified, PerkinElmer) was infused at a rate of 0.05 μCi/min for 2 h to assess the basal glucose turnover, and a hyperinsulinemic-euglycemic clamp in awake mice was conducted for 140 min with a primed/continuous infusion of human insulin (126 pmol/kg prime, 18 pmol/kg/min infusion) (Eli Lilly). During the clamp, plasma glucose was maintained at basal concentrations (~6.7 mM). Rates of basal and insulin-stimulated whole-body glucose fluxes and tissue glucose uptake were determined after a bolus (10 μCi) injection of 2-deoxy-D-[1-^{14}C]glucose (2-DOG) (PerkinElmer), as previously described (18).

194 ***Lipidomics Analyses***

195 For lipid analyses, internal standards (C17:0 cer, C19: 0–19:0 DAG, or C17:0 acyl-CoA,
196 respectively) were added to plasma (1 mM, 20 μl each) or liver homogenates (20 mg each) samples.
197 Ceramide was extracted from the samples by addition of chloroform and methanol (2:1), as described
198 previously (19); collected organic phase was evaporated under N_2 gas and the residue was
199 reconstituted in 100 μl 0.1% formic acid in methanol, and was subjected to LC/MS/MS analysis.
200 Separately, the lipid extract was run on silica thin-layer chromatography. Phospholipids were scraped
201 and the composition of FAs and phospholipids was measured using GC/MS technique (20). For
202 analyses of sphingolipid, electrospray ionization mode was used in the positive mode as described
203 previously (21, 22).
204
205 ***Human Samples***

206 The NAFLD liver specimens were obtained from the University of Kansas Liver Center Tissue
207 Bank between 2010 and 2011 (cohort #1) and Division of Digestive and Liver Diseases, Department
208 of Medicine, Comprehensive Transplant Center, Cedars-Sinai Medical Center in 2017 (cohort #2). All
209 of the procured specimens received proper patient consents with approval from each Institutional
210 Review Board (#00042709 for cohort #2). For cohort #1, the subjects included 17 males and 16
211 females, at the average age of 51.1±2.4 and the liver biopsies from those diagnosed with normal
212 (n=15), steatosis (n=12) or steatohepatitis (n=6) were analyzed. For cohort #2, the liver specimens,
213 being reviewed and scored using H&E-stained sections by pathologists in a blinded fashion, from
214 subjects with clinical diagnosis of normal (n=5), simple steatosis (n=3) or NASH (n=2) were analyzed
215 for immunoblottings.
216
217 ***Adenosine Measurements***

218 To obtain the serum and liver homogenate samples from mice, as much blood as possible was
219 collected via the heart puncture, and each mouse was then sacrificed by cervical dislocation. Liver

was excised, weighed and homogenized with a 4-fold volume of normal saline. After centrifugation for 10 min, the supernatant was collected. Adenosine concentrations in sera or liver homogenates were measured using UPLC-MS/MS, as previously described with modifications (23). A 30 μl serum and liver samples were used for the sample preparation steps. A 60 μl of 50 ng/ml phenacetin in acetonitrile was added as an internal standard to each serum or liver homogenate sample. After centrifuging at 12,000 rpm for 10 min, a 5 μl of the supernatant was injected onto UPLC-MS/MS system. To extinguish the endogenous adenosine and measure the spiked concentration of exogenous adenosine in sera and liver homogenates, the samples were kept for 24 h at room temperature to completely degrade endogenous adenosine, and then a known concentration of adenosine and ADA inhibitors [100 μM of dipyridamole and 2.5 μM of erythro-9-(2-hydroxy-3-nonyl)adenine] were added. Quantitation was achieved by MS/MS detection using Waters UPLC-XEVO TQ system (Waters Corporation, Milford). The mass transitions for adenosine and phenacetin were *m/z* 268.01 → 135.86 (collision energy, 15 eV) and 179.96 → 110.01 (20 eV), respectively, in the multiple reaction monitoring (MRM) mode with positive ionization. These compounds were separated on a reversed-phase C_{18} column (ACQUITY UPLC 2.1 mm × 100 mm i.d., 1.7-μm particle size; Waters, Ireland) with a flow rate of 0.3 ml/min. The mobile phase composition was started at 10:90 (v/v) of acetonitrile and distilled water containing 0.1% formic acid and gradually changed to 90:10 (v/v) for 2 min, and held 2.5 min, and then switched back to 10:90 (v/v) for 2.6 to 4.5 min.

Transient Transfection

Scrambled control siRNA, or siRNA specifically directed against $G\alpha_{12}$, HIF-1α, and USP22 were purchased from Santa Cruz Biotechnology (Santa Cruz, CA). The transfection with siRNA (100 nM) was carried out using FuGENE® HD Reagent (Roche, Indianapolis, IN) in accordance with manufacturer's procedure.

Establishment of Stable Cell Lines

To generate $G\alpha_{12}$-depleted stable cell lines, either shRNA-expressing plasmid against mouse $G\alpha_{12}$

(sh-Gα_{12}) or non-targeting luciferase as a control (sh-Luci) was transfected into AML12 cells using FuGENE® HD Reagent (Roche, Indianapolis, IN) in accordance with manufacturer's procedure, and stably transfected cells were selected using puromycin (2 μg/ml, Thermo Fisher Scientific, Logan, UT) (2).

RNA Isolation and qRT-PCR Assays

Total RNA was extracted using Trizol (Invitrogen, Carlsbad, CA) and was reverse-transcribed. The resulting cDNA was amplified by qRT-PCR as previously described (2). β-Actin or GAPDH was used as normalization control. The primer sequences used for qRT-PCR assays were provided in Supplemental Table 1.

Immunoblot Analysis

SDS-polyacrylamide gel electrophoresis and immunoblot analyses were performed according to previously published procedures (1).

Immunoprecipitation Assay

To assess SIRT1 ubiquitination, HepG2 cells were infected with Ad-Gα_{12}QL (or Ad-Con) for 6 h, followed by subsequent transfection with a plasmid encoding His-tagged ubiquitin (His-Ubi) in Eagle's minimum essential medium containing 1% fetal bovine serum (FBS) for 24 h, and continuously incubated with 20 μM MG132 for 6 h. Cell lysates were incubated with anti-SIRT1 antibody overnight at 4°C. After immunoprecipitation, the antigen-antibody complex was precipitated following incubation for 2 h at 4°C with protein G-agarose. The immune complex was solubilized in 2×Laemmli buffer and boiled for 5 min. The samples were immunoblotted with anti-ubiquitin antibody.

Reporter Gene Assays

The upstream promoter region of mouse *Usp22* gene containing up to -2.2 kb was cloned into the pGL3 luciferase vector. A mutation of HRE in the mouse gene was done by deleting the sequence of putative HIF-1α binding element (5'-(A/G)CGTG-3') located between -539 bp and -535 bp (Mut1); or between -287 bp and -283 bp (Mut2), respectively. Cells were transfected with pGL3-USP22 for 12 h with either Mock or $G\alpha_{12}QL$ plasmid in the presence of FuGENE® HD reagent, and luciferase activity was measured by adding luciferase assay reagent (Promega, Madison, WI).

Statistics

Values are expressed as mean± standard error of mean (SEM). Statistical significance was tested by two-tailed Student's *t* test or 1-way ANOVA with Bonferroni or Least Significant Difference (LSD) multiple comparison procedure where appropriate. Differences were considered significant at $P < 0.05$.

Supplementary References

1. Kim TH, et al. An active metabolite of oltipraz (M2) increases mitochondrial fuel oxidation and inhibits lipogenesis in the liver by dually activating AMPK. *Br J Pharmacol.* 2013;168(7):1647-1661.
2. Yang YM, et al. Galpha12 gep oncogene deregulation of p53-responsive microRNAs promotes epithelial-mesenchymal transition of hepatocellular carcinoma. *Oncogene.* 2015;34(22):2910-2921.
3. Mi H, et al. PANTHER version 11: expanded annotation data from Gene Ontology and Reactome pathways, and data analysis tool enhancements. *Nucleic Acids Res.* 2017;45(D1):D183-d189.
4. Huang da W, et al. Bioinformatics enrichment tools: paths toward the comprehensive functional analysis of large gene lists. *Nucleic Acids Res.* 2009;37(1):1-13.
5. Huang da W, et al. Systematic and integrative analysis of large gene lists using DAVID bioinformatics resources. *Nat Protoc.* 2009;4(1):44-57.
6. Franceschini A, et al. STRING v9.1: protein-protein interaction networks, with increased coverage and integration. *Nucleic Acids Res.* 2013;41(Database issue):D808-815.
7. Shannon P, et al. Cytoscape: a software environment for integrated models of biomolecular interaction networks. *Genome Res.* 2003;13(11):2498-2504.
8. Yang YM, et al. Decrease of microRNA-122 causes hepatic insulin resistance by inducing protein tyrosine phosphatase 1B, which is reversed by licorice flavonoid. *Hepatology.* 2012;56(6):2209-2220.
9. Vogt S, et al. Receptor-dependent RhoA activation in G12/G13-deficient cells: genetic evidence for an involvement of Gq/G11. *J Biol Chem.* 2003;278(31):28743-28749.
10. Frezza C, et al. Organelle isolation: functional mitochondria from mouse liver, muscle and cultured fibroblasts. *Nat Protoc.* 2007;2(2):287-295.
11. Deberardinis RJ, et al. Phosphatidylinositol 3-kinase-dependent modulation of carnitine palmitoyltransferase 1A expression regulates lipid metabolism during hematopoietic cell growth. *J Biol Chem.* 2006;281(49):37372-37380.
12. Buzzai M, et al. The glucose dependence of Akt-transformed cells can be reversed by pharmacologic activation of fatty acid beta-oxidation. *Oncogene.* 2005;24(26):4165-4173.
13. Shin KJ, et al. A single lentiviral vector platform for microRNA-based conditional RNA interference and coordinated transgene expression. *Proc Natl Acad Sci U S A.* 2006;103(37):13759-13764.
14. Sowa ME, et al. Defining the human deubiquitinating enzyme interaction landscape. *Cell.* 2009;138(2):389-403.
15. Pinkert CA, et al. An albumin enhancer located 10 kb upstream functions along with its promoter to direct efficient, liver-specific expression in transgenic mice. *Genes Dev.*

1987;1(3):268-276.

16. Yang YM, et al. Metadoxine, an ion-pair of pyridoxine and L-2-pyrrolidone-5-carboxylate, blocks adipocyte differentiation in association with inhibition of the PKA-CREB pathway. *Arch Biochem Biophys.* 2009;488(2):91-99.

17. Wu HM, et al. Mitigation of carbon tetrachloride-induced hepatic injury by methylene blue, a repurposed drug, is mediated by dual inhibition of GSK3beta downstream of PKA. *Br J Pharmacol.* 2014;171(11):2790-2802.

18. Kim KH, et al. Autophagy deficiency leads to protection from obesity and insulin resistance by inducing Fgf21 as a mitokine. *Nat Med.* 2013;19(1):83-92.

19. Bligh EG, and Dyer WJ. A rapid method of total lipid extraction and purification. *Can J Biochem Physiol.* 1959;37(8):911-917.

20. Magnes C, et al. LC/MS/MS method for quantitative determination of long-chain fatty acyl-CoAs. *Anal Chem.* 2005;77(9):2889-2894.

21. Yoo HH, et al. Liquid chromatography-tandem mass spectrometric determination of ceramides and related lipid species in cellular extracts. *J Chromatogr B Analyt Technol Biomed Life Sci.* 2006;843(2):327-333.

22. Lee SY, et al. Activation of sphingosine kinase 2 by endoplasmic reticulum stress ameliorates hepatic steatosis and insulin resistance in mice. *Hepatology.* 2015;62(1):135-146.

23. Sharma K, et al. Highly sensitive method for the determination of adenosine by LC-MS/MS-ESI: method validation and scope of application to a pharmacokinetic/pharmacodynamic study. *Biomed Chromatogr.* 2012;26(1):81-88.

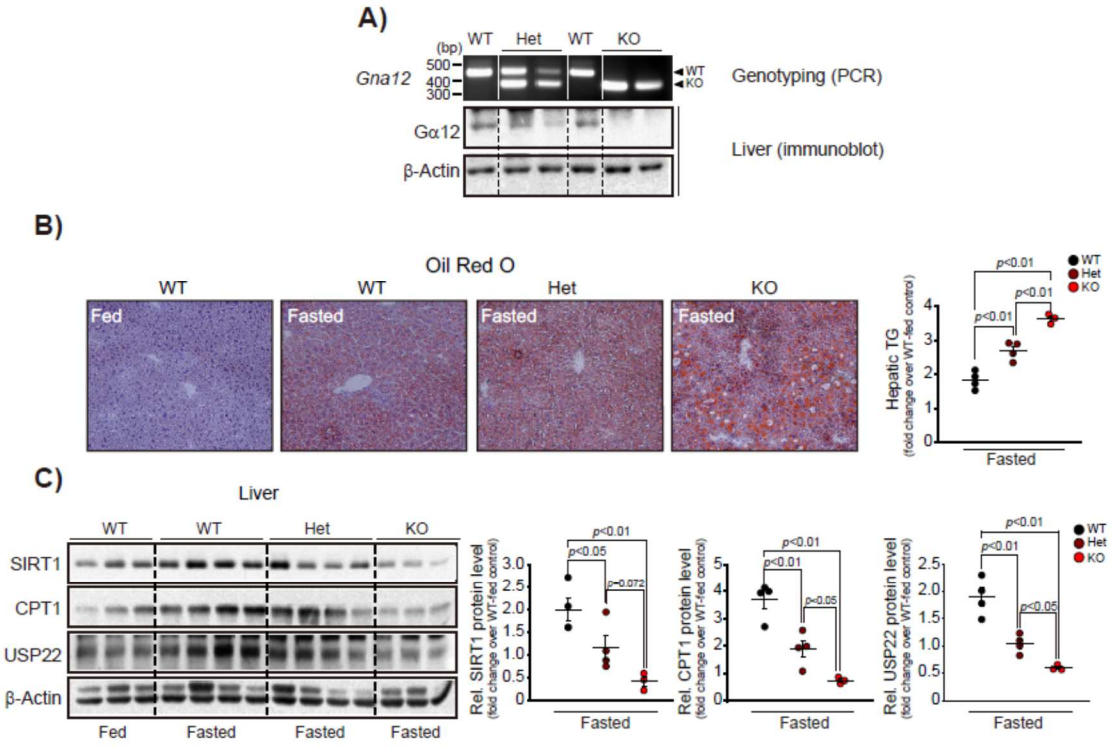

Fig. S1

Supplemental Figure 1. The partial phenotype of heterozygous for *Gna12* deficiency on SIRT1 induction and hepatic steatosis by fasting

(**A**) PCR analysis for *Gna12* in genomic DNA isolated from the tails of WT (littermates), heterozygous for *Gna12* deficiency (Het), and *Gna12* KO mice (upper). Immunoblotting assay for $G\alpha_{12}$ was done using liver homogenates prepared from same mice (lower).

(**B**) Representative Oil Red O staining (left, original magnification ×20), and TG contents (right) in the liver tissues. Mice at 14 weeks of age were subjected to fasting for 24 h (n=3-4/group).

(**C**) The effect of heterozygous deletion of *Gna12* on fasting induction of SIRT1. Immunoblottings for SIRT1, CPT1, and USP22 (left) in the liver homogenates from the above mice, and their respective quantifications (right) (n=3-4/group).

Values represent the mean ± SEM. Data were analyzed by ANOVA followed by Bonferroni (**B**) or LSD (**C**) post hoc tests. For **B** and **C**, only fasted groups were analyzed for ease of data presentation. For **A** and **B**, the blots in each panel were run in parallel using same samples and β-actin was used as a normalization control for densitometric analysis.

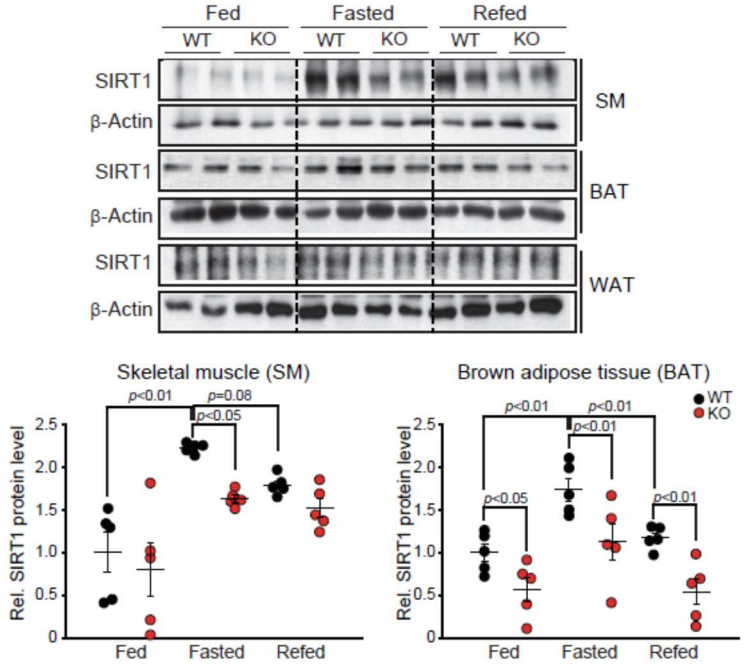

Fig. S2

Supplemental Figure 2. Lack of adaptive SIRT1 induction by fasting in extrahepatic tissues of *Gna12* KO mice

Abrogation of SIRT1 induction upon fasting by *Gna12* KO. Immunoblottings for SIRT1 were done on the homogenates of skeletal muscle (SM), brown adipose tissue (BAT), or white adipose tissue (WAT) from 12-week-old mice fed ND ad libitum, followed by fasting and re-feeding for 24 h (n=5/group). Values represent the mean ± SEM. Data were analyzed by ANOVA followed by LSD post hoc test. The blots were run in parallel using same samples and β-actin was used as a normalization control for densitometric analysis.

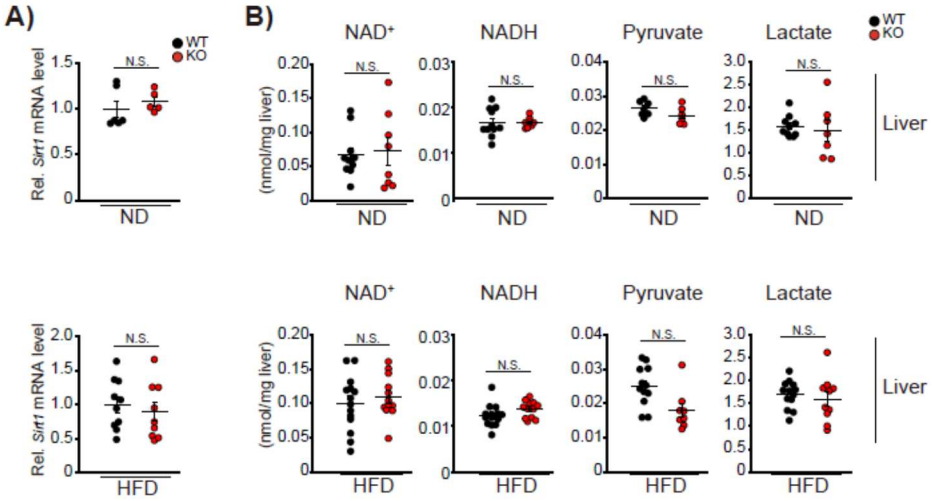

Fig.S3

Supplemental Figure 3. The effects of *Gna12* KO on SIRT1 regulation

(**A**) qRT-PCR assays for *Sirt1* in the liver of WT or *Gna12* KO mice fed either ND (upper) or HFD (lower) (n=5-10/group).

(**B**) The contents of NAD^+, NADH, pyruvate, and lactate in the liver of mice as described in **A** (n=6-14/group).

For **A** and **B**, values represent mean ± SEM. N.S., not significant

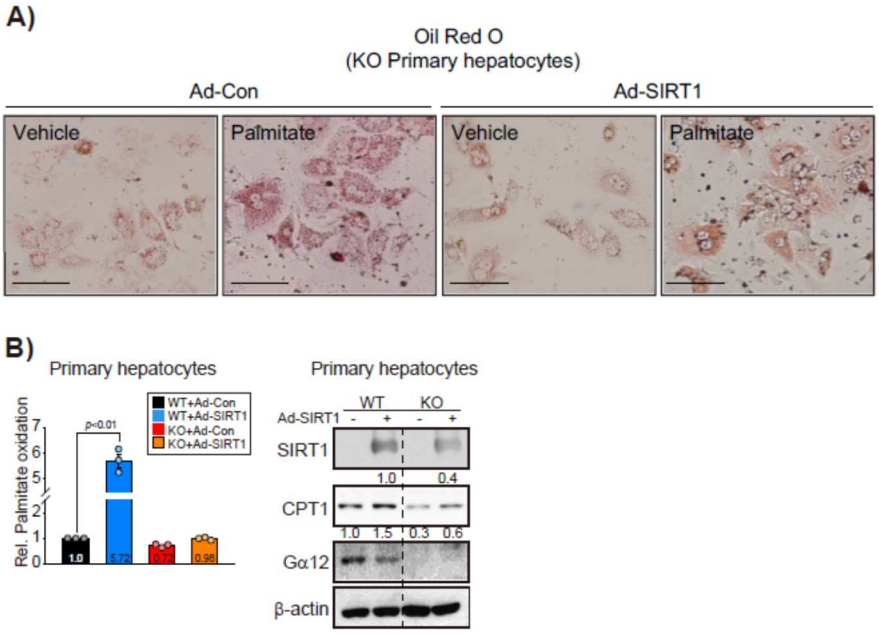

Fig.S4

Supplemental Figure 4. The effect of SIRT1 overexpression on lipid accumulated in *Gna12* KO hepatocytes

(**A**) Representative Oil Red O staining in *Gna12* KO primary hepatocytes (n=2-3/group). After infection with Ad-SIRT1 (or Ad-Con) for 10 h, the cells were treated with 500 μM palmitate (or BSA control) for 18 h. Scale bar, 50 μm

(**B**) Palmitate oxidation in primary hepatocytes. The [^{3}H]-palmitate oxidation rate was determined in WT or *Gna12* KO primary hepatocytes infected with Ad-SIRT1 (or Ad-Con) as in **A** (left, n=3; values indicate mean). Immunoblottings for SIRT1 and CPT1 were done using the lysates prepared from the assay (right; the values were shown as relative band intensity). The blots were run in parallel using same samples and β-actin was used as a normalization control for densitometric analysis.

For **B**, values represent mean ± SEM. Data was analyzed by ANOVA followed by LSD post hoc test.

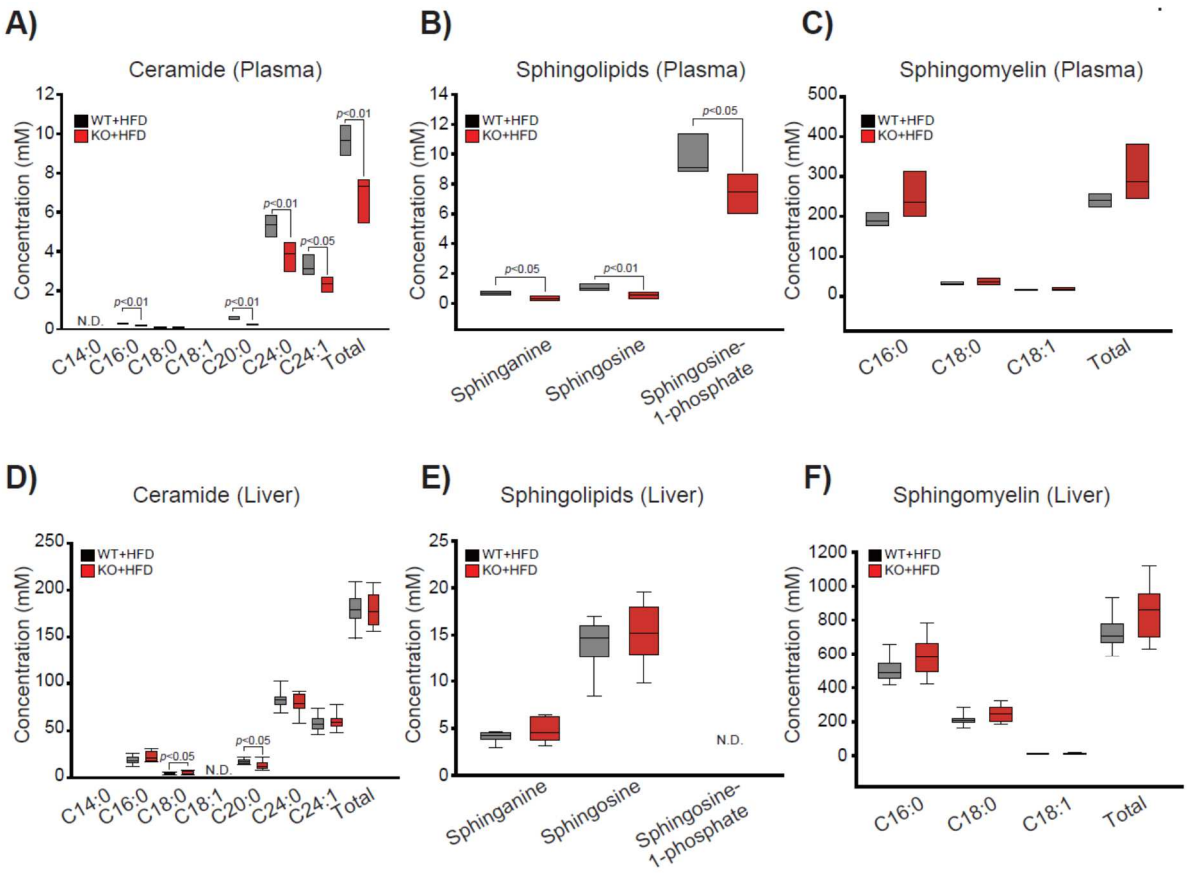

Fig.S5

Supplemental Figure 5. Lipidomic analyses of plasma and liver samples from WT or *Gna12* KO mice.

(**A**-**F**) The samples were collected from WT and *Gna12* KO mice fed HFD for 16 weeks. The contents of ceramides (**A**, **D**), sphingolipid bases (sphinganine, sphingosine, and sphingosine 1-phosphate) (**B**, **E**), and sphingomyelin (**C**, **F**) were measured using LC-MS/MS method (n=5/group for plasma; n=9-10/group for liver).

For **A**-**F**, values represent mean ± SEM. Data were analyzed by two-tailed Student's *t* test. Box-and-whisker plots show median (horizontal lines within boxes), 5-95% percentile (the bounds of the boxes), and range of minimum to maximum values (whiskers).

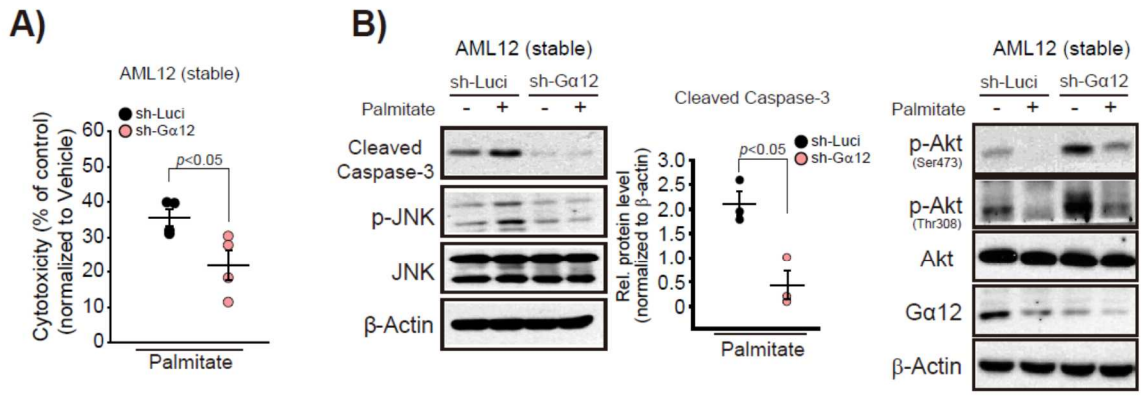

Fig.S6

Supplemental Figure 6. The effect of $G\alpha_{12}$ gene knockdown on the viability of AML12 cells treated with palmitate

(**A**) Cell viability assay. AML12 cells stably expressing sh-$G\alpha_{12}$ (or sh-Luci) were treated with 500 μM palmitate for 48 h, and cell viability was analyzed by MTT assay. The result shown represents four independent experiments (n=4-6 replicates/group for each experiment).

(**B**) Immunoblottings for cell death-related markers. AML12 cells stably expressing sh-$G\alpha_{12}$ (or sh-Luci) were treated with 500 μM palmitate for 36 h. The blots were run in parallel using same samples and β-actin was used as a normalization control for densitometric analysis of cleaved caspase-3 (middle, n=3).

Values represent mean ± SEM. Data were analyzed by two-tailed Student's *t* test (**A** and **B**).

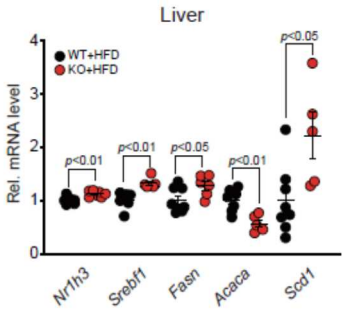

Fig.S7

Supplemental Figure 7. The effects of *Gna12* KO on lipogenic gene expression

qRT-PCR assays for lipogenic genes in the liver of mice as described in Figure 7F (n=5-8/group). Values represent mean ± SEM. Data were analyzed by two-tailed Student's *t* test.

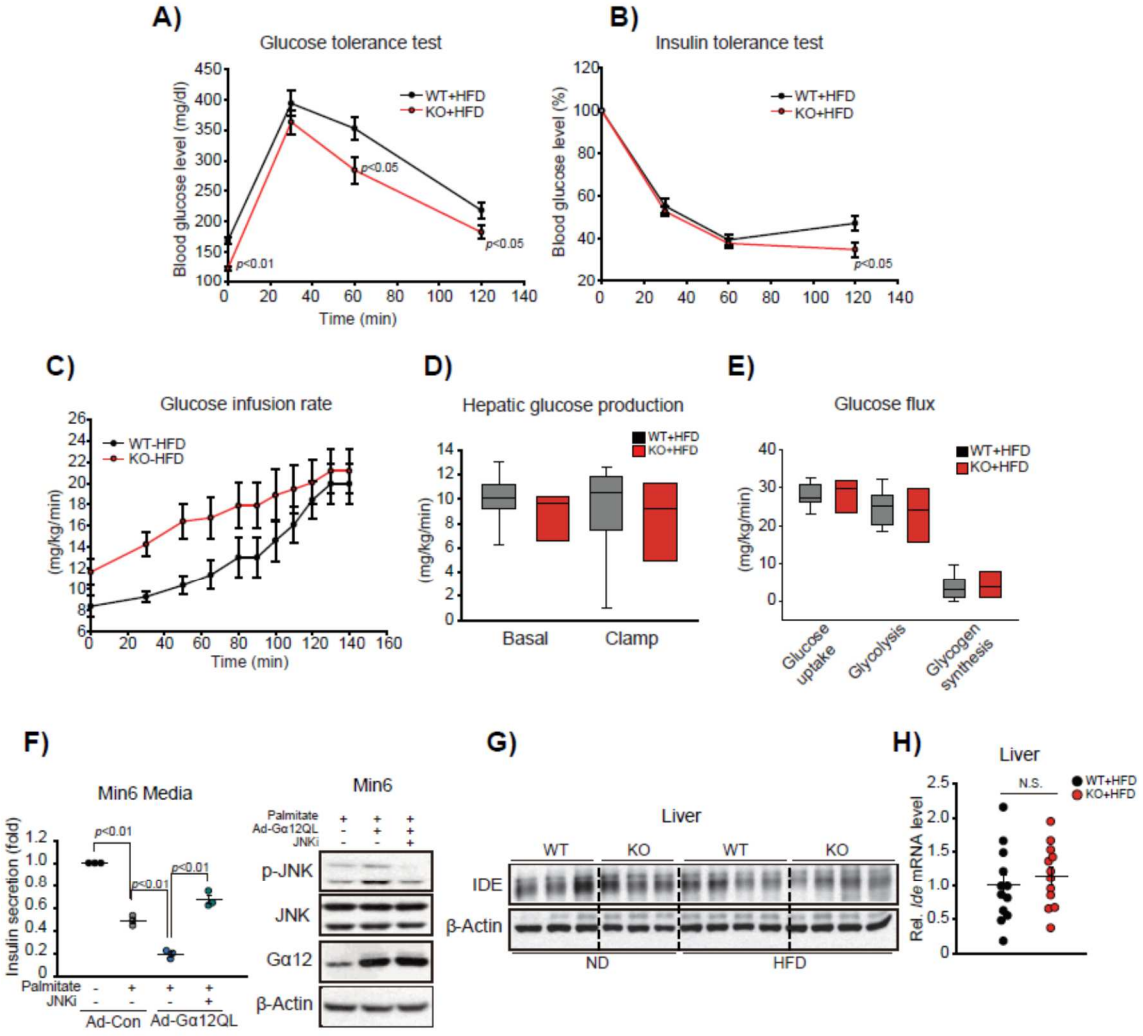

Fig.S8

Supplemental Figure 8. The effect of *Gna12* KO on glucose metabolism

(**A**) Glucose tolerance tests. Eight-week-old WT or *Gna12* KO mice fed HFD for 13 weeks were subjected to blood glucose measurements (n=9-10/group).

(**B**) Insulin tolerance tests. WT and *Gna12* KO mice were fed HFD for 15 weeks (n=12-14/group).

(**C**) Glucose infusion rates. Hyperinsulinemic-euglycemic clamp was conducted on WT or *Gna12* KO mice fed HFD for 6 weeks (n=7-9/group).

(**D**) Hepatic glucose production rates in the same mice as in **C** (n=7-9/group).

(**E**) Glucose flux comprising glucose uptake, glycolysis, and glycogen synthesis in the same mice as in **C** (n=7-9/group).

(**F**) Glucose-stimulated insulin secretion assay. Min6 cells infected with Ad-Gα_{12}QL (or Ad-Con) were treated with 500 μM palmitate with or without chemical JNK inhibitor (SP600125, 20 μM) for

24 h, followed by stimulation with high glucose (25 mM, 1 h). The content of insulin secreted into the culture media for each sample was measured by ELSIA assay and was normalized to cellular protein concentration (left). The ELISA result represents three independent experiments (n=4 replicates/group for each experiment). Immunoblottings were done using cell lysates prepared from the assay (right).

(**G**) Immunoblotting for IDE in the liver of WT or *Gna12* KO mice fed either ND or HFD for 16 weeks.

(**H**) qRT-PCR assay for *Ide* in the liver of mice as in **G** (n=12/group).

Values represent the mean ± SEM. Data were analyzed by two-tailed Student's *t* test (**A** and **B**) or ANOVA followed by Bonferroni (**F**) post hoc test. For **D** and **E**, box-and-whisker plots show median (horizontal lines within boxes), 5-95% percentile (the bounds of the boxes), and range of minimum to maximum values (whiskers). For **F** and **G**, the blots were run in parallel using same samples. N.S., not significant

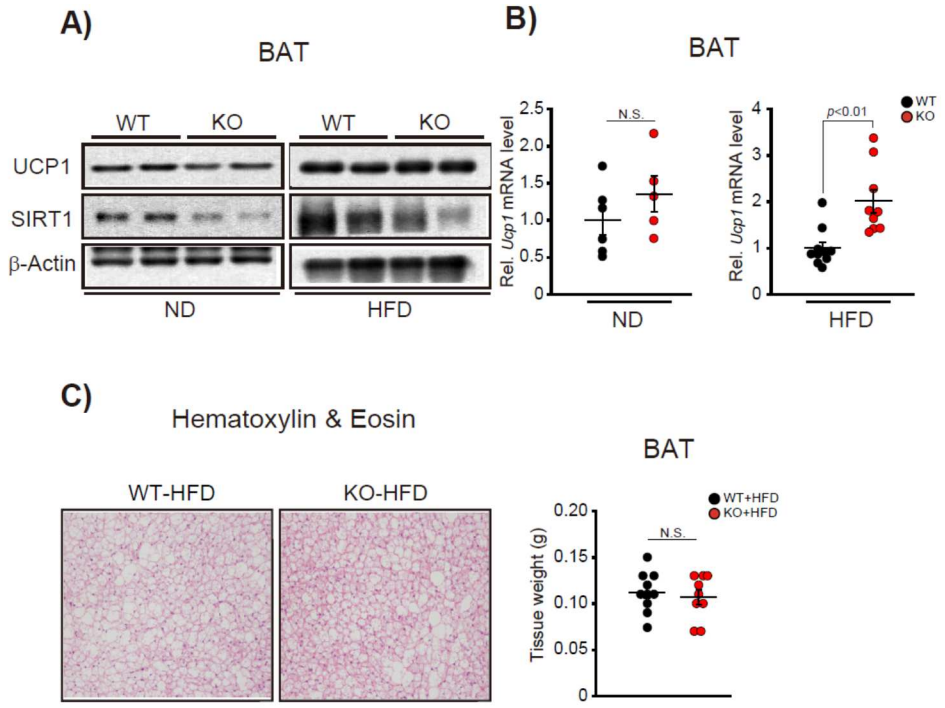

Fig.S9

Supplemental Figure 9. The effects of *Gna12* KO on the genes in brown adipose tissue

(**A**) Immunoblottings for UCP1 and SIRT1 in the homogenates of brown adipose tissue (BAT) from WT or *Gna12* KO mice fed either ND or HFD for 16 weeks. The blots were run in parallel using same samples.

(**B**) qRT-PCR assays for *Ucp1* in the above samples (n=5-10/group).

(**C**) Representative H&E staining of BAT (left, n=3/group), and tissue weights (right, n=9-10/group).

Values represent mean ± SEM. Data were analyzed by two-tailed Student's *t* test (**B**). N.S., not significant

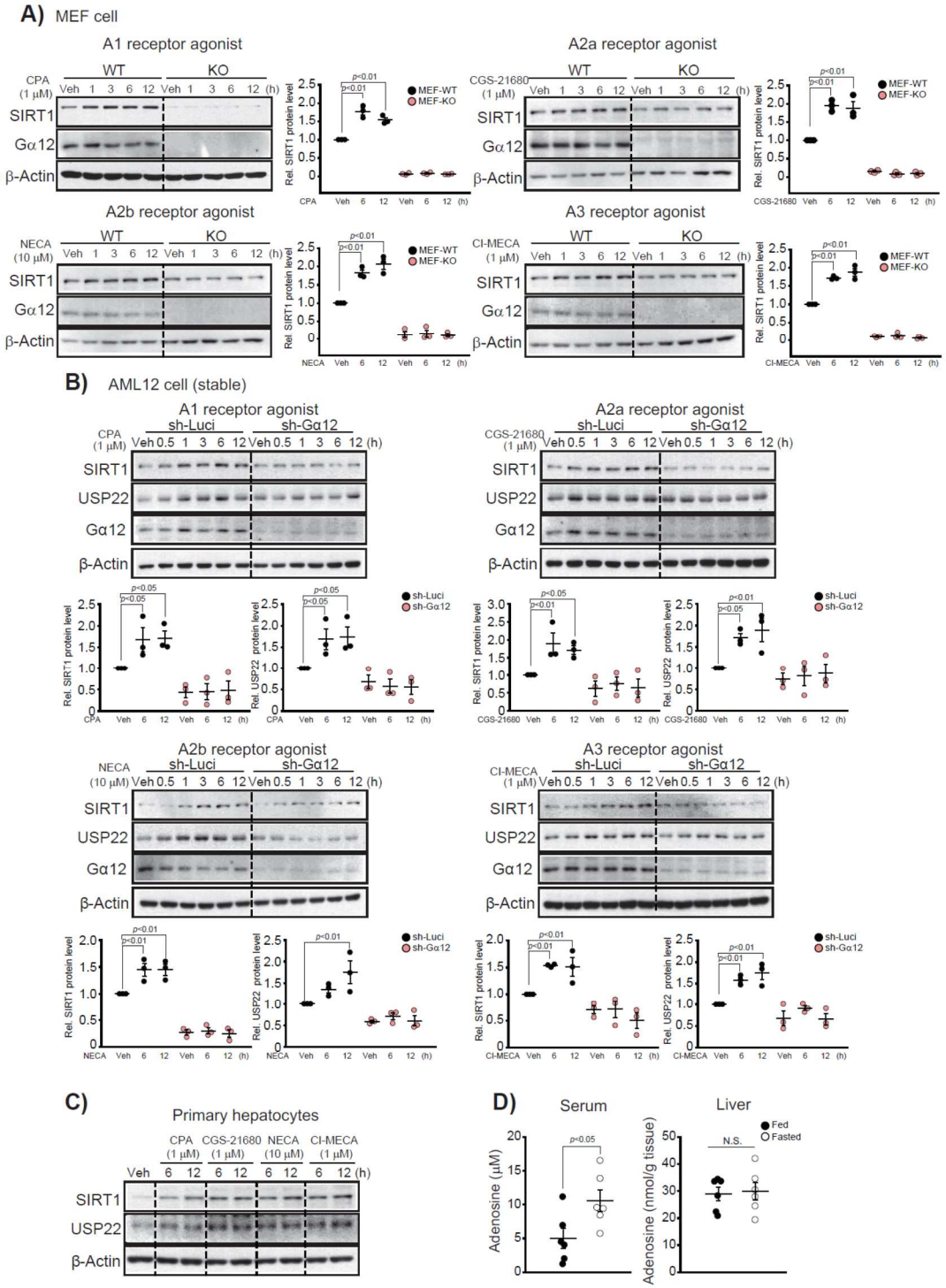

Fig.S10

Supplemental Figure 10. The role of Gα$_{12}$ in the induction of SIRT1 by adenosine signaling

(**A**) Immunoblottings for SIRT1 in MEF cells treated with each agonist for adenosine receptors (CPA, 1 μM; CGS-21680, 1 μM; NECA, 10 μM; and Cl-IB-MECA, 1 μM) for the indicated times (left), and their respective quantifications (right, n=3/group).

(**B**) Immunoblottings for SIRT1 and USP22 in AML12 cells stably expressing shRNA against Gα$_{12}$

(sh-Gα_{12}) or control luciferase (sh-Luci) treated with reagents as in **A** (upper), and their respective quantifications (lower, n=3/group).

(**C**) Immunoblottings for SIRT1 and USP22 in mouse primary hepatocytes treated with reagents as in **A**.

(**D**) Adenosine concentrations in sera or liver homogenates from WT mice fasted for 24 h (n=6/group). Values represent mean ± SEM. Data were analyzed by ANOVA followed by LSD (**A** and **B**) post hoc test or two-tailed Student's *t* test (**D**). For **A**-**C**, the blots were run in parallel using same samples and β-actin was used as a normalization control for densitometric analysis. N.S., not significant

492 Supplemental Table 1. The sequences of primer pairs for qRT-PCR assays

Gene names	Pairs	Primer sequences (mouse)
ACC (Acetyl-CoA carboxylase)	sense	5′-GTCAGCGGATGGGCGGAATG-3′
	anti-sense	5′-CGCCGGATGCCATGCTCAAC-3′
β-actin	sense	5'-CTGAGAGGGAAATCGTGCGT-3'
	anti-sense	5'-TGTTGGCATAGAGGTCTTTACGG-3'
CD36	sense	5′-GATGACGTGGCAAAGAACAG-3′
	anti-sense	5′-TCCTCGGGGTCCTGAGTTAT-3′
CPT1	sense	5′-GTCGCTTCTTCAAGGTCTGG-3′
	anti-sense	5′-AAGAAAGCAGCACGTTCGAT-3′
FAS (Fatty acid synthase)	sense	5′-AGCGGCCATTTCCATTGCCC-3′
	anti-sense	5′-CCATGCCCAGAGGGTGGTTG-3′
GAPDH (Glyceraldehyde-3-phosphate dehydrogenase)	sense	5’-AACGACCCCTTCATTGAC-3’
	anti-sense	5’-TCCACGACATACTCAGCAC-3’
IDE (Insulin degrading enzyme)	sense	5′-AGCTCCTGTGTGTCACTTGG-3′
	anti-sense	5′-CACTTGCGGAAGCCTGAGTA-3′
Acadl (Acyl-Coenzyme A dehydrogenase, long chain)	sense	5-GCATCAACATCGCAGAGAAA-3’
	anti-sense	5-GGCTATGGCACCGATACACT-3’
LPL (Lipoprotein lipase)	sense	5’-CCCTACAAAGTGTTCCATTA-3’
	anti-sense	5’-CTCGCTCTCGGCCACTGT-3’
LXRα (Liver X receptor)	sense	5′-TGCCATCAGCATCTTCTCTG-3′
	anti-sense	5′-GGCTCACCAGCTTCATTAGC-3′
Acadm (Acyl-Coenzyme A dehydrogenase, medium chain)	sense	5'-TTGAGTTGACGGAACAGCAG-3'
	anti-sense	5'-CCCCAAAGAATTTGCTTCAA-3'
PGC1α	sense	5′-ACGAGGCCAGTCCTTCCTCC-3′
	anti-sense	5′-AGCTCTGAGCAGGGACGTCT-3′
PPARα	sense	5′-CGGGAAAGACCAGCAACAAC-3′
	anti-sense	5′-TGGCAGCAGTGGAAGAATCG-3′
PPARγ	sense	5'-GTTTTATGCTGTTATGGGTG-3'
	anti-sense	5'-GTAATTTCTTGTGAAGTGCT-3'
PPARδ	sense	5'-CGGACCTGGGGATTAATGGG-3'
	anti-sense	5'-ATGGACTGCCTTTACCGTGG-3'
SCD1 (Stearoyl-CoA desaturase-1)	sense	5′-CCGGAGACCCTTAGATCGA-3′
	anti-sense	5′-TAGCCTGTAAAAGATTTCTGCAAACC-3′
SIRT1	sense	5'-CAGTGTCATGGTTCCTTTGC-3'
	anti-sense	5'-CACCGAGGAACTACCTGAT-3'
SREBP-1 (Sterol regulatory element binding protein-1)	sense	5′-AACGTCACTTCCAGCTAGAC-3′
	anti-sense	5′-CCACTAAGGTGCCTACAGAGC-3′
UCP1 (Uncoupling protein 1)	sense	5'-CTGGGCTTAACGGGTCCTC-3'
	anti-sense	5'-CTGGGCTAGGTAGTGCCAGT-3'
USP22	sense	5'-TCTACCAGTGCTTCGTGTGG-3'

	anti-sense	5'-CATGGTCATGGATGTGCTTC-3'

493